MSc in Photonics

PHOTONICS**BCN**

Universitat Politècnica de Catalunya (UPC)
Universitat Autònoma de Barcelona (UAB)
Universitat de Barcelona (UB)
Institut de Ciències Fotòniques (ICFO)

http://www.photonicsbcn.eu

Master in Photonics

MASTER THESIS WORK

BEAM STEERING ACCURACY IN HOLOGRAPHIC OPTICAL TWEEZERS

Frederic Català i Castro

Supervised by Dr. Estela Martín Badosa, (UB)

Presented on date 10th September 2013

Registered at

Escola Tècnica Superior d'Enginyeria de Telecomunicació de Barcelona

Beam steering accuracy in holographic optical tweezers

Frederic Català i Castro
Optical Trapping Lab – Grup de Biofotònica (BiOPT), Dept. de Física Aplicada i Òptica, Universitat de Barcelona, c/ Martí i Franquès, 1, 08028 Barcelona (Spain)

E-mail: frederic.catala@gmail.com

Abstract. The use of spatial light modulators (SLMs) to achieve dynamic control of optical tweezers is observed to provide subnanometer precision in single trap positioning. However, some features concerning the digitalized structure of SLMs cause a loss of precision in certain kinds of experiments. In this work, positioning accuracy of holographic optical tweezers (HOTs) is profoundly analysed in these cases, and a correction methodology is proposed in order to improve trap positioning.

Keywords: wavefront modulation, digital holography, optical trapping, bead tracking.

1. Introduction

The possibilities provided by optical tweezers in the manipulation of specimens at the micron and sub-micron scale have been widely investigated since their discovery in 1970 [1]. The use of devices such as acousto-optic deflectors (AODs) or galvano mirrors has allowed a dynamic positioning of the traps. Compared to these solutions, holographic optical tweezers (HOTs) offer useful and novel capabilities derived from beam shape engineering: creation of multiple optical traps in 3D, aberration compensation and generation of exotic light beams, among others. In particular, the use of spatial light modulators (SLMs) for wavefront shaping can be applied to accurate beam steering and, therefore, to precise positioning of optical traps [2-3]. However, the digital structure of SLMs reduces the ability of undertaking continuous modulation of phase, thus decreasing steering accuracy [4-5]. In addition, the unavoidable error made in the linkage between the 8-bit signal and the real phase applied locally to the beam at each pixel of the SLM is an important aspect that must be taken into account, when addressing the phase distribution of the hologram.

The purpose of this investigation is to analyse and understand these undesirable effects and their impact on the precision in trap positioning, which was obtained by tracking trapped polystyrene microbeads. After the optimization of hologram computation, we were able to perform and measure subnanometer holographic trap displacements.

The work is structured as follows: in section 2, imprecisions in beam steering accuracy, due to the SLM digital performance are quantified analytically; in section 3, we describe the employed set-up and the techniques developed to SLM phase characterization and microbead tracking measurements; finally, in section 4, measurements of the incorrectness of trap positioning in particular cases are shown, as well as our capability to rectify them.

2. Holographic steering

Beam steering execution using SLM is based on the ability to modify the phase of the wavefront locally. This provides a way to yield a certain deflection up to a maximum angle that depends on the SLM pixel width and the wavelength (See figure 1). In the particular case of creating an optical trap with a microscope objective, the incoming plane wave is focused into a point, whose displacement with respect to the center is straightforwardly related to the slope applied to

the wavefront at the SLM and the objective focal length. Besides, two distinguished traps can be created because SLMs typically modulate only one of the two independent linear polarizations of the beam. Therefore, the trap corresponding to the modulated polarization is steered wherever, whereas the other one remains unaltered at the optical axis.

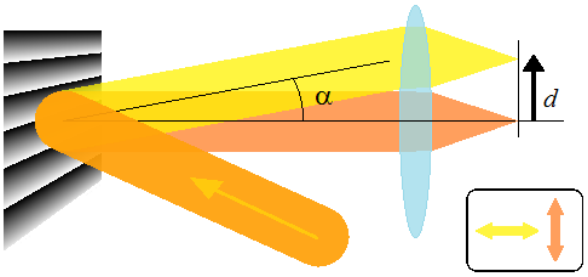

Figure 1. An incoming beam is split into two independently polarized beams after the SLM. While one of them is modulated and thereby steered a certain angle, the other one is reflected as if the SLM was a plane surface.

While ideal beam steering lies in the capability to modulate the wavefront continuously in space, and allowing any point of the wavefront to take continuous phase values from 0 to 2π, the digital arrangement of SLMs, i.e. pixelation of space and quantization of phase values, lowers both the steering efficiency and accuracy [4-5]. Furthermore, non-precise relationship between the electronically addressed gray levels and the realized phase values might lead to a worse wavefront modulation as well. This is the reason why an analysis of the SLM look-up-table (LUT) needs to be performed, as will be demonstrated in section 3.2. Two solutions are proposed to overcome imprecise beam steering regarding both the phase quantization and LUT effects.

2.1. SLM digitalization aspects

The conventional way to compute the holograms to be displayed at the SLM consists in associating, at each pixel, the closest phase value available with respect to the ideal one at the center of the pixel. The ideal phase value that an analog 1D SLM should provide at the jth pixel in order to steer the beam to an angle α is given by

$$\phi_j^{ideal}(\alpha) = \frac{2\pi}{\lambda} x_j \sin\alpha + \phi_0 \quad [1]$$

where x_j is the center coordinate of the pixel, and $j=1,...,N$, being N the number of pixels. Parameter ϕ_0 produces, at first, no effect on the deflection angle, although we will see that some variations can be produced by setting it in a proper way during the phase quantization process. Since there are only M equidistant phase values between 0 and 2π, the final expression for the phase distribution will be

$$\phi_j(\alpha) = round\left[\phi_j^{ideal}(\alpha)\frac{M}{2\pi}\right]\frac{2\pi}{M} \quad [2]$$

From now on, we can consider the mean slope of the realized modulation staircase to be the actual steering angle. It can be easily calculated by adjusting a linear fit to the modulation staircase. This way, we are able to see that phase values quantization tend to produce deflection angles slightly different from the aimed, as shown in figure 2(a). Moreover, we can see that adding the offset phase ϕ_0 might induce some changes in the overall phase distribution, in spite of producing no effect on the wavefront slope in the ideal analog performance, as shown in figure 2(b).

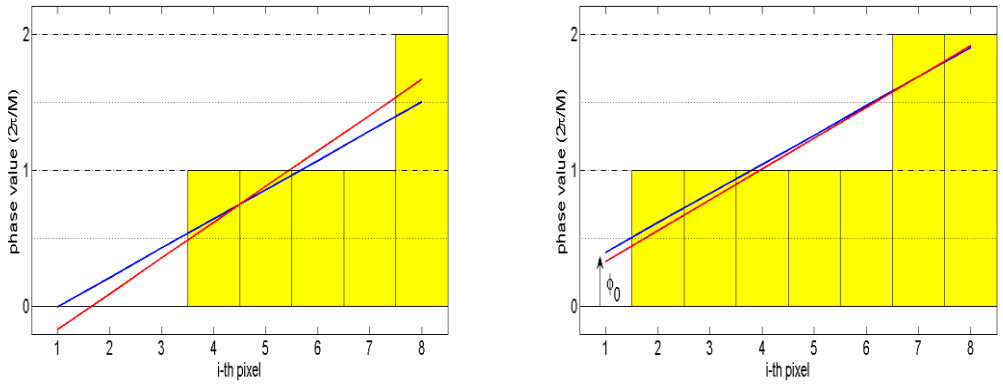

(a) (b)

Figure 2. In both figures, the blue line corresponds to the ideal phase distribution given by expression 1. The yellow bar plot regards the phase quantized actual hologram, and the red line is the linear fit to it, whose slope coincides with the actual beam deflection angle. Observe, in (a), that the aimed and the realized angles differ considerably, whereas the addition of ϕ_0, represented in (b), can reduce this difference. Note that the blue lines in both figures have got the same slope but different intercept.

It is worth to comment on the fact that ϕ_0 should be a *fractional* gray level, i.e. phase values not corresponding to $2\pi/M$, $2\cdot 2\pi/M$, …, $(M-1)\cdot 2\pi/M$, otherwise no change on the mean slope would be induced even after the phase values quantization. In fact, adding a non-integer offset to the ideal phase profile can make some pixels overtake the phase threshold and take another gray level, whereas other pixels remain unchanged, and the mean slope of the staircase can thereby vary, as shown in figure 2(b). The offset ϕ_0 will always be considered to take values continuously between 0 and 1, i.e. the first gray level.

On the other hand, there are some steering angles that will be perfectly reproduced as they coincide with slopes that are equal to an integer number of gray levels per pixel. Thereby, adding an offset ϕ_0 will only yield changes in the intercept of the linear fit of the staircase, but not in the slope. Positions regarding these angles are consequently named $d^{(n)}_{match}$ in equation [3]. Although these positions are perfectly achieved, steering accuracy gets largely worse around them, if no ϕ_0 optimization is considered. Observe its behavior in figure 3.

$$d^{(n)}_{match} = n\frac{\lambda f}{m p} \quad [3]$$

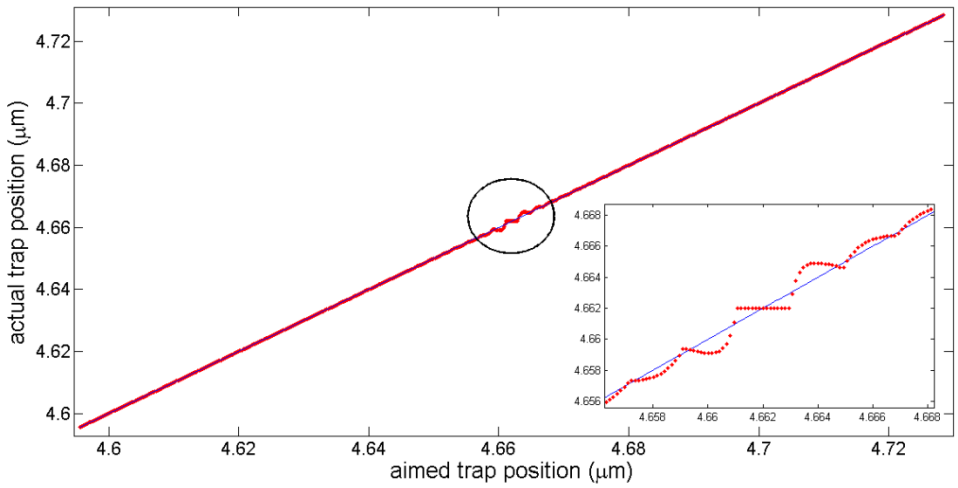

Figure 3. Simulation of the realized positioning of the trap around $d^{(4)}_{match}$. Observe that accuracy is considerably degenerated in the nearest regions of $d^{(4)}_{match}$.

In section 4, the effect of adding a global phase offset in trap positioning will be shown. However, the prediction based on the mean slope method does not coincide with the real positioning perfectly. The fact that our actual problem is bidimensional, as well as the point that the entrance pupil is circular and the objective works with high NA, are the main causes for this lack of coincidence. Therefore, steering optimization must be carried out by finding experimentally the ϕ_0 values that make the actual positioning to be as similar to the aimed as possible.

3. Experimental methodology

3.1. Set-up description

The optical tweezers set-up used in our experiments is represented in figure 4. The employed laser is a continuous-wave (CW) type that emits a Gaussian beam TEM_{00} up to 5W at a wavelength of 1064nm. A combination of a half wave-plate and a polarizing beam splitter facilitates power control by polarization. The SLM in our set-up is a Hamamatsu X10468-03. After a first telescope that widens the beam so that it is adapted to the SLM dimensions, another half wave-plate is placed in order to rotate the polarization, hence giving a way to control the relative power of the modulated beam (x-polarization) with respect to the non-modulated beam (y-polarization). In our *dumbbell* configuration, both traps must have the same power, thus the half wave-plate must rotate polarization up to 45º. A second telescope conjugates the SLM plane at the entrance pupil of the objective with a certain magnification in order to fit its size. The objective is a NIKON 60x working at NA 1.2 at maximum conditions in water immersion, and focuses the incoming laser light into the specimen to create the optical trap.
From the other side of the sample, a condenser illuminates the specimen from above, and its image through the objective is registered at the CCD placed at the NIKON microscope desired port after passing through a dichroic mirror.

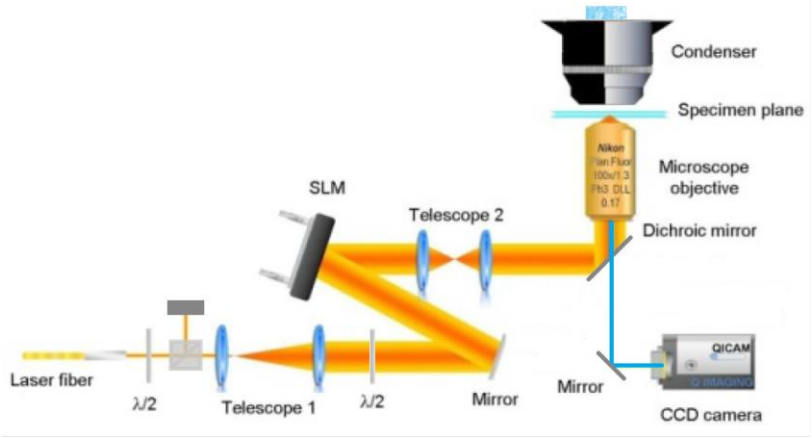

Figure 4. The set-up consists mainly of an objective that focuses the laser beam in order to create the optical trap, after being modulated by the SLM, and an imaging layout consisting of a condenser and a CCD camera.

3.2. SLM characterization

As has been mentioned, phase modulation is achieved for only x-polarized light. If the phase modulating profile is a linear slope, an x-polarized beam will be steered a desired angle, while a y-polarized beam will be reflected as if the SLM was a plane surface. However, if the phase modulating profile is a constant gray level, even the modulated field component is commonly reflected as well, i.e. undergoing no additional steering. Therefore, the incoming beam is no longer split into two beams, but polarization of the actual single beam depends on the phase delay between both field components. This provides a way to figure out the correspondence between the gray levels and the actual modulation phase applied to the beam.

A 45º linearly polarized beam was shone onto the SLM, which applied a certain gray level homogeneously. A photodetector recorded the intensity of the beam after passing through an analyzer at -45º. When no phase delay is produced at the SLM, light intensity drops down to a minimum, since it remains linearly polarized at 45º; whereas a phase delay of 180º makes light intensity reach its maximum. In the intermediate cases, elliptically polarized light is produced. A scheme of the measurement procedure is shown in figure 5.

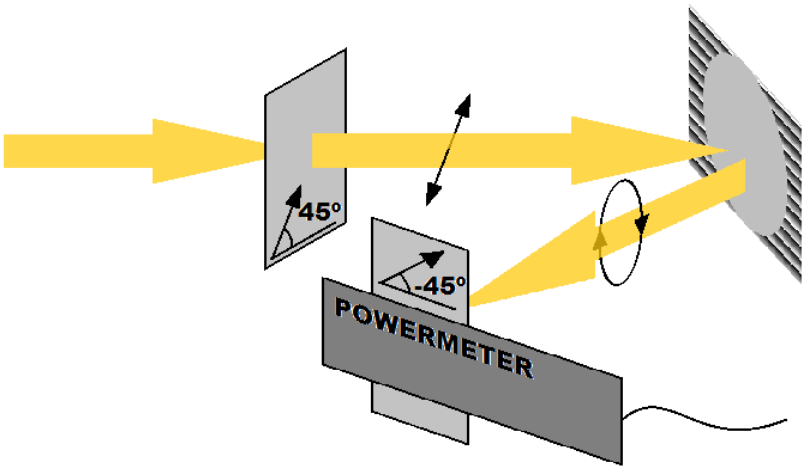

Figure 5. Set-up employed to characterize the phase modulation by the SLM. The light intensity recorded at the photodetector depends on the resulting light polarization after the modulator, i.e. the phase that has been yielded onto one of the field components.

The homogeneous gray level was applied over the circle inscribed into the narrowest direction of the SLM, whereas the remaining regions of the hologram were programmed to steer residual light out. This way, we obtain the characterization of the region of the SLM that fits the entrance pupil of the objective, and therefore, the area that creates the optical trap.
A software developed in LABVIEW carried out a sweep over all the grey levels and plotted curves as shown in figure 6, as well as fitted the *sine square* model in expression 4. The parameter T tells us the number of gray levels between 0 and 2π, and thus coincides with the quantization number M in expression 2. On the other hand, parameter g_0 provides an additional degree of freedom that may take a global shift into account; which might be caused by a constant phase delay of the non-modulated component of polarization. Parameters I_0 and A inform about the offset intensity measured by the photodetector and the peak-to-peak relation of the signal, although they are not relevant in our SLM characterization method.

$$I(g) = I_0 + A\ \sin^2\left[\frac{\pi}{T}(g - g_0)\right] \quad [4]$$

The high linearity of our SLM, shown in figure 6, allows us to apply the *look-up-table* by only fixing the value of M properly. The gray period was observed to get wider as power was increased, and a non-linear behavior was observed to start at a laser power of about 2W. In order to create traps powerful enough to minimize Brownian motion, all the experiments were carried out at a laser power of 1.5W, for which the gray period M was assessed a value of 228.

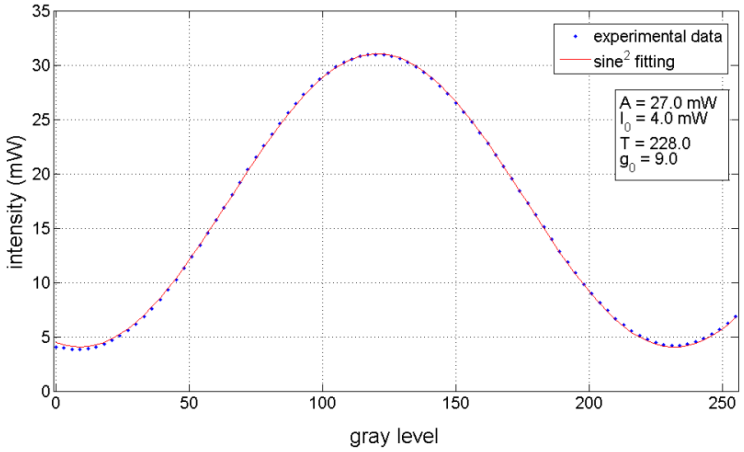

Figure 6. The intensity response depends on the modulation in phase undergone by one of the polarization components of the beam. Notice the agreement between the experimental result and the theoretical model.

3.3. Bead tracking method

We used 1μm sized polystyrene beads to be captured at both traps, and their position was precisely measured by means of the tracking software Video Spot Tracker developed by CISMM – UNC Nanoscale Science Research Group [6]. An infrared filter was placed before the CCD camera not to merge the laser light with the illumination.

Tracking of two beads facilitates a way to subtract drift effects that can be due to air fluctuations among other experimental issues, which will affect both traps equally since they go through the same optical path in the set-up. A noticeable drift motion cancelation is shown in figure 7(a). Furthermore, a digital filter is applied in order to minimize the Brownian motion of the beads.

All in all, the LABVIEW program was set to change automatically the position of the holographic trap, in order to analyze its positioning accuracy along the axis of interest. The mean position and its standard deviation were calculated over a certain time while the trap was motionless, but allowing margin enough so that transitory effects were avoided, as shown in figure 7(b). Finally, after removing Brownian and drift effects, we reached position measurements within an error bar of about ±0.3 nm, which is in accordance with rigorous statistical analysis developed in Allan-variance calculations [7].

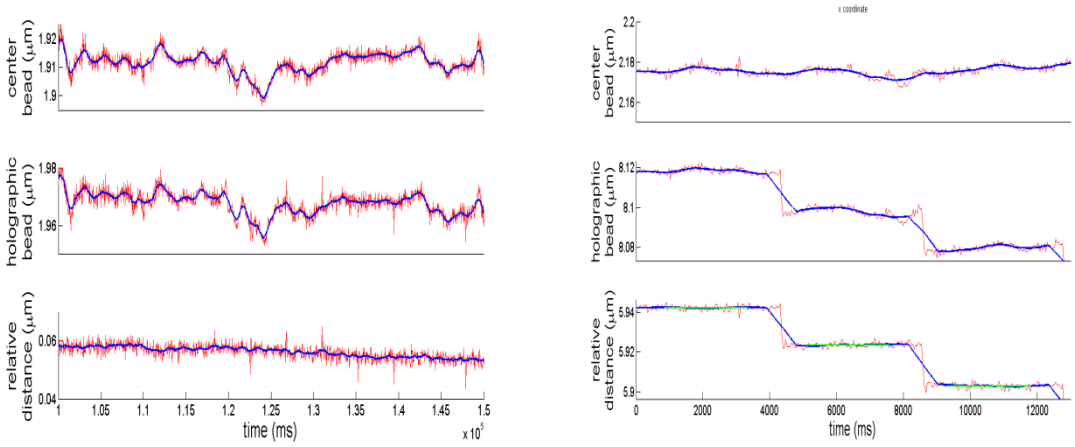

(a) (b)

Figure 7. In both figures, the red line is the direct bead tracking measurement, while the blue one is the result of applying a digital filter to cancel Brownian motion. As you can see in (a), after removing it, both beads undergo a parallel behavior that is largely eliminated by calculating the respective position one another. In figure (b), an example of sequential positioning is shown, where the green line in the figure below represents the time during which the mean relative position and standard deviation are calculated.

It is important to notice that actual trap positions measured by bead tracking may not coincide exactly with the aimed, even in the case that wavefront modulation was performed ideally. The main reason for this is the fact that the laser that creates the trap, and the imaging system, go through different optical elements thereupon the dichroic mirror below the objective, and this results in a presumable mismatch in the respective optical magnifications, that has been assessed to be 3%. That is to say, measurements show that traps are created a 3% nearer to the centre. Nevertheless, this can be easily overcome by comparing the actual trap position to the linear fit that adjusts a certain number of points, as can be shown in the figures of the next section.

4. Results

Several tracking experiments have been carried out in the way described above, in two different ranges. At the *nanoscale* range, trap positioning errors due to phase quantization in the wavefront modulation are observed and corrected by optimizing ϕ_0. At the *microscale* range, positioning inaccuracies are analysed and a correction method is proposed.

4.1. Nanoscale range

As mentioned in section 2.1, positioning accuracy is much worse around certain points called $d^{(n)}_{match}$, and ϕ_0 optimization needs to be carried out around them. A measurement in the region of $d^{(4)}_{match}$ is shown in figure 8(a) and results to be quite similar to the simulation in figure 3. Observe that positioning errors up to 2 nm occur in the nearest zone of $d^{(4)}_{match}$, whereas accuracy is considerably ameliorated as the trap is created a few nanometers away. In fact, notice that far enough from $d^{(4)}_{match}$, we are able to realize 0.2 nm steps with an average error that is less than 0.4 nm, hence positioning is mostly achieved within the error bars. On the other hand, the effect of adding a fractional ϕ_0 offset, for a certain aimed position, is shown in figure 8(b).

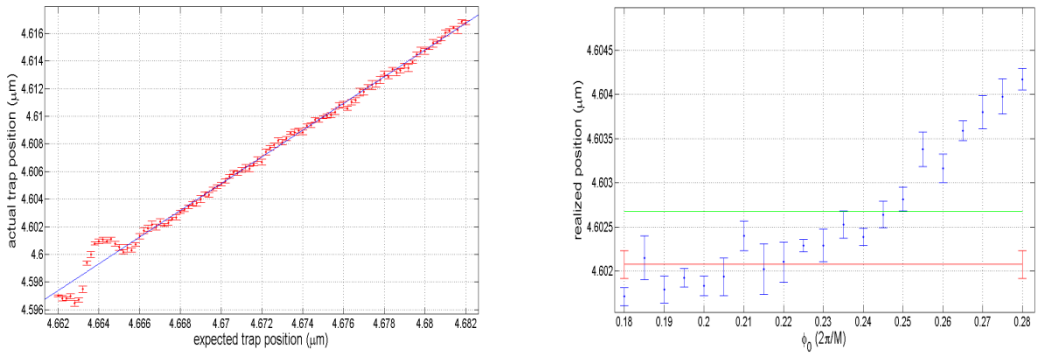

(a) (b)

Figure 8. (a) Measurement around $d^{(4)}_{match}$. Observe the inaccuracy yielded in the adjacent zone of $d^{(4)}_{match}$, whereas the proper position sampling in the more distant regions. (b) Effect of adding a fractional ϕ_0 offset to the overall hologram; red: $d^{(4)}_{match}$; green: expected trap position; blue: reached positions for each ϕ_0.

The procedure performed in order to assess the ϕ_0 optimization values consists in obtaining measurements as that shown in figure 8(b) for each position –it has been realized at every 0.2 nm from $d^{(4)}_{match}$=4.662nm to 4.665nm-. The ϕ_0 value that leads to the best positioning is then set to be added automatically in further hologram computations. Observe, in figure 9, that the errors produced in the optimized experiment become much smaller, down to less than 1 nm.

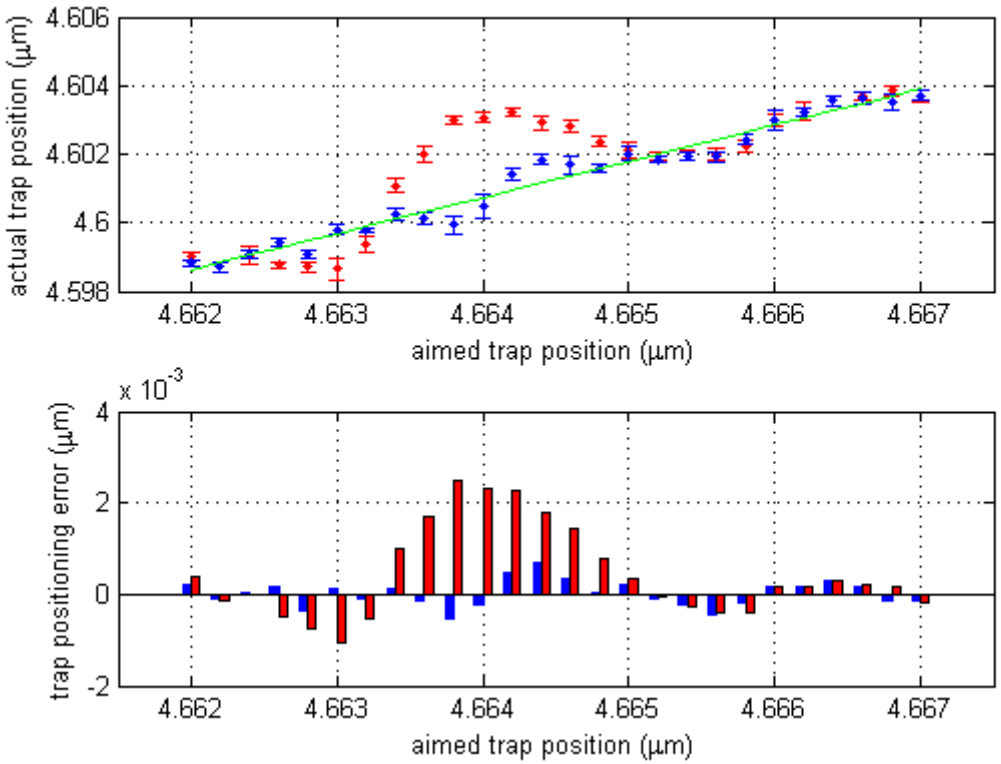

Figure 9. In the graphic above, we plot the actual positioning before (red) and after (blue) applying the ϕ_0 correction. Below, the errors with respect to the aimed trap position (green line in the plot above) are represented.

4.2. Microscale range

Apart from the digitalization effects studied in earlier sections, other kind of inaccuracies were noticed when realizing steps at the microscale range, i.e. steps of about 0.1 μm, as shown in figure 10. To be sure that phase quantization did not affect the holographic modulation, these bead tracking experiments were realized at $d^{(n)}_{match}$ positions defined in expression 3, i.e. those positions that are properly achieved intrinsically, because no ϕ_0 addition produces any modification in trap positioning. Thereby, inaccuracies in our experiments are not due to wrong kinoform computing, but are caused by other experimental phenomena. The fact that the SLM look-up-table has been considered to be linear by only setting properly the parameter *M* might be one of the main reasons for this imprecise trap location. However, one notices it only when carrying out experiments at the microscale, because consecutive holograms differ substantially one another. On the other hand, when performing experiments at the nanoscale, the relative movement of the trap is correctly realized, because holograms remain considerably unchanged throughout the tracking experiments.

At the same time, we observed that adding a global *integer* phase, named ψ_0 not to be confused with the *fractional* ϕ_0 employed in the previous optimization method, yields positioning variations that can be taken in advantage in order to optimize accuracy. The addition of such a ψ_0 phase leads to a remarkable shift of the kinoform sawtooth, whereas summing a fractional ϕ_0 phase produces an almost identic hologram in which a few pixels may vary up to 1 gray level, because a different rounding is achieved, as has been discussed in section 2.1. The result of adding the phase ψ_0 to the hologram is shown in figure 11.

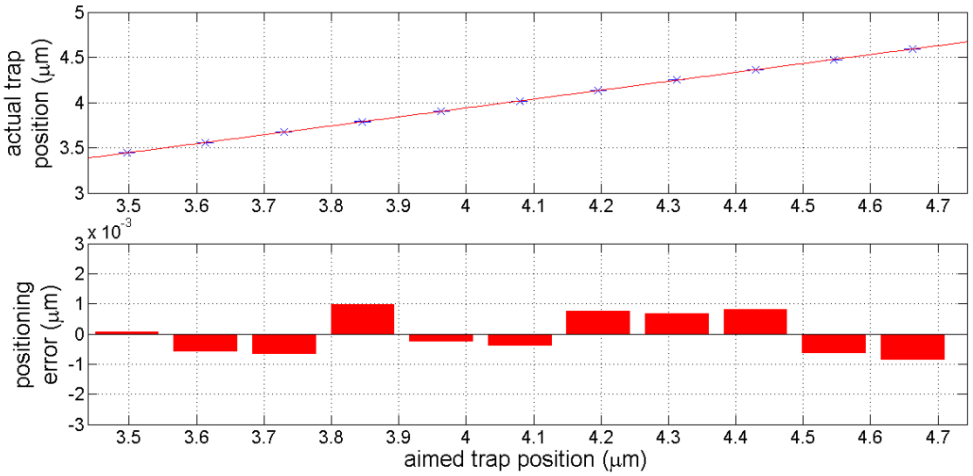

Figure 10. Measured trap positions from $d^{(3)}_{match}$=3.4965μm to $d^{(4)}_{match}$=4.662μm (above). Observe below the residuals of the actual positions with respect to the linear fit that adjusts the entire tracking. Note that errors up to 1 nm are produced if holograms are computed straightforwardly.

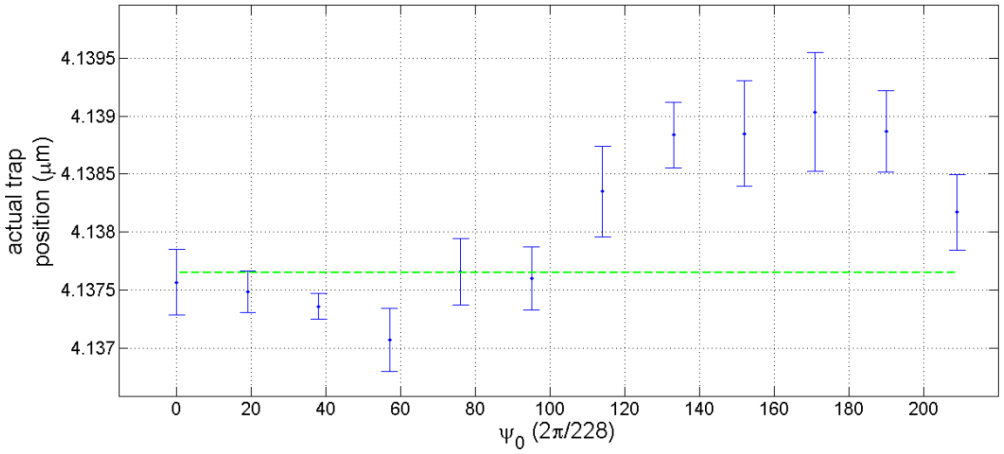

Figure 11. Evolution of trap positioning by adding an integer phase offset, which leads to a hologram lateral shift (blue). Note that variations of 2 nm are yielded this way. In green, the expected trap position with respect to a previous position of the trap.

5. Conclusions

One of the most important results in the experiments we have described is the fact that the bead tracking method allows measurements with subnanometer precision. This technique, consisting in trapping two beads to cancel drift effects and filtering the signals digitally to eliminate the Brownian motion, provides the capability to analyse the loss of accuracy, due to the digital performance of SLMs, that occur at certain positions of the sample, named $d^{(n)}_{match}$. In the case of working with 228 gray levels, the inaccuracy produced is about 2 nm, and the tracking method is precise enough to observe it.

At nanoscale experiments, we performed and were capable to measure 0.2 nm steps and found that they were realized with typical errors similar to the error bars, in positions according to correct beam steering. On the other hand, around $d^{(n)}_{match}$ positions, the tracking showed clearly that trap positioning is not achieved in an appropriate way. We rectified the imprecisions due to holographic effects by means of the ϕ_0 offset method and errors smaller than 1 nm were achieved.

At microscale experiments, we observed another kind of inaccuracy that is not related to digitalization issues at the SLM, because measurements were specifically undertaken at exactly

$d^{(n)}_{match}$ positions. This incorrectness is due to considerable changes in the hologram performance, in contrast to the fact that holograms remained almost static when carrying out experiments at nanoscale. This is the reason why a sequence of constant steps of about 100 nm was found to vary slightly and take errors of about 1 nm.
However, the point that shifting laterally the kinoform by means of adding a global integer phase, named ψ_0, produces modifications in trap positioning, can be taken in advantage to correct this inaccuracy. Moreover, noticing that shifting the hologram produce changes in beam steering agrees with the hypothesis that the observed inaccuracies at microscale are due to large changes in the hologram structure.
To conclude, two kinds of inaccuracies in trap positioning are yielded in holographic optical tweezers. While digitalized beam modulation effects are observed at the nanoscale, the lack of robustness of the look-up-table of the SLM is observed at the microscale. Finally, both imprecisions can be solved in similar ways. While the first one is overcome by adding fractional phases that readjust the gray levels in order to produce staircase mean-slopes as similar to the aimed as possible, the second one lies in adding integer large phases that lead to a hologram lateral shift.

Acknowledgments
I would like to express my gratitude to my advisor, Prof. Estela Martín-Badosa for her help and encouragement throughout the course of this work, as well as Arnau Farré, Ferran Marsà and Josep Mas for the countless amount of advice and aid all along the months this master thesis has been performed.

References
[1] A. Ashkin, "Acceleration and trapping of particles by radiation pressure", Phys. Rev. Letters **24**, 156-159 (1970)
[2] A. Horst, N. Forde, "Calibration of dynamic holographic optical tweezers for force measurements on biomaterials", Opt. Express, **16**, 20987-21003 (2008)
[3] C. H. J. Smith, J. P. Spatz, J. E. Curtis, "High-precision steering of multiple holographic optical traps", Opt. Express, **13**, 8678-8685 (2005)
[4] D. Engström, J. Bengtsson, E. Eriksson, M. Goksör "Improved beam steering accuracy of a single beam with a 1D phase-only spatial light modulator", Opt. Express, **22**, 18275-18287 (2008)
[5] Lingjiang Kong, Ying Zhu, Yan Song, Jianyu Yang, "Beam steering approach for high-precision spatial light modulators", Chinese Optics Letters, **8**, 1085-1089 (2010)
[6] http://cismm.cs.unc.edu/resources/software-manuals/video-spot-tracker-manual
[7] F. Cerwinski, A. C. Richardson, L. B. Oddershede, "Quantifying Noise in Optical Tweezers by Allan Variance", Opt. Express, **17**, 13255-13269 (2009)